




Cite this: *Mater. Adv.*, 2022,
3, 6019

A solution-derived bismuth aluminum gallium tin oxide film constructed by a brush coating method for spontaneous liquid crystal alignment

Dong Wook Lee,^a Eun Mi Kim,^b Gi Seok Heo,^b Dong Hyun Kim,^a Jin Young Oh,^a
Dae-Hyun Kim,^c Yang Liu^{*d} and Dae-Shik Seo ^{*a}

We present a facile liquid crystal (LC) alignment method using brush hairs. This one-step brush coating method integrated film deposition and alignment layer treatment, which guarantees a high throughput. Bismuth aluminum gallium tin oxide (BiAlGaSnO) was used for the alignment layer, and a uniform and homogeneous LC alignment state was confirmed for a 280 °C cured brush coated film by polarized optical microscopy and pretilt angle analysis. X-ray photoelectron spectroscopy was used to verify the formation of the BiAlGaSnO layer on the glass substrate. Atomic force microscopy confirmed the oriented structure on the BiAlGaSnO surface induced by the shear stress of brush movement and active thermal oxidation via the curing process. This anisotropic surface derives the uniform LC alignment via geometric constraints under the boundary condition of the interface with the LCs. The BiAlGaSnO surface exhibited hydrophilicity with a nanocrystalline structure in contact angle and selected area diffraction analyses. The thermal stability of the BiAlGaSnO film to LC alignment was confirmed up to 150 °C from the annealing process. The good electro-optical performance of the BiAlGaSnO film was also verified by the fast switching characteristics. Based on the above results, the brush coating method is expected to be an effective strategy for next-generation LC applications.

Received 15th April 2022,
Accepted 15th June 2022

DOI: 10.1039/d2ma00421f

rsc.li/materials-advances

1. Introduction

Liquid crystals (LCs) are interesting materials that exhibit optical and dielectric anisotropies.^{1–3} Based on their unique characteristics, LC devices and LC displays (LCDs) play important roles in the advancement and development of the electronic and display industries, due to their long-term durability, excellent resolution, and good electro-optical (EO) performances such as a fast response time (RT) and a low operating voltage, which result in low power consumption.^{4–7} To ensure high performance, uniform LC alignment is considered as an important criterion.^{8,9} The LC alignment property is affected by the alignment layer property as well as interactions between the LC and alignment layers via physicochemical processes. To fabricate

the alignment layer, film deposition is performed first, for which various thin-film deposition methods have been studied and reported, such as atomic layer deposition,¹⁰ sputtering,¹¹ chemical vapor deposition,¹² and solution processing. Specifically, solution processing is related to film crystallization and controllability of orientation properties, which are useful for advanced functional device applications.^{13–15} Solution processing can also be adopted for high-function LC devices. It is ecofriendly, requires low-temperature processing, and has highly reliable characteristics that are needed for next-generation technologies. Solution processing includes various coating methods, such as bar coating,¹⁶ dip coating,¹⁷ blade coating,¹⁸ and brush coating.^{19–21} In particular, the brush coating method has the distinct property of adjusting the surface orientation of the molecules during the coating process using the shear stress from the solution affected by the brush hair movements.

After film deposition, various alignment processing techniques are generally required to align the LC molecules on the film, including ultraviolet photoalignment,²² plasma treatment,²³ and rubbing.^{24,25} Specifically, the rubbing method has been used conventionally in various industries. This method uses the microgroove effect (originating from the mechanical contact between the spinning fabric and the deposited thin film) to uniformly align the LC molecules. However, it has several limitations, such as cracks on the surface, because of mechanical contact with the fabric rotating at a high speed and large-area processing, leading to high cost.²⁶

^a IT Nano Electronic Device Laboratory, Department of Electrical and Electronic Engineering, Yonsei University, Seodaemun-gu, Seoul 120-749, South Korea.
E-mail: dsseo@yonsei.ac.kr

^b National Center for Nanoprocess and Equipment, Korea Institute of Industrial Technology, 6 Cheomdangwagi-ro 208beon-gil, Buk-gu, Gwangju 500-480, South Korea

^c Department of Smart Electric, Korea Polytechnic, 23, Yeomjeon-ro, 333beon-gil, Nam-gu, Incheon 22121, South Korea

^d College of Information Science and Technology, Donghua University, 2999 North Renmin Road, Songjiang District, Shanghai 201620, China.
E-mail: liuyang@dhu.edu.cn

Herein, we adopted a brush coating method for uniform LC alignment that can handle the additional effects of the rubbing process and reduce the process steps by integrating film deposition and alignment treatment. As mentioned above, the brush coating process produces oriented structures from the shear during the solution deposition process; hence, we expect that this method can also guarantee a high throughput. Bismuth aluminum gallium tin oxide (BiAlGaSnO) was adopted because of the good EO properties of its components^{27–30} and was produced *via* the sol-gel process before being used for the alignment layer owing to the high EO properties of the components. The LC alignment state on the BiAlGaSnO film was investigated by polarized optical microscopy (POM) and pretilt angle analysis. The surface orientation property of the film was examined by atomic force microscopy (AFM), and X-ray photoelectron spectroscopy (XPS) was used to measure the chemical components of the film to confirm the good formation of the BiAlGaSnO layer. Contact angle measurements were obtained to investigate the surface chemical affinity. The crystalline properties of the film were examined by X-ray diffraction (XRD) and transmission electron microscopy selected area diffraction (TEM-SAD). Thermal characterization of BiAlGaSnO was examined by differential scanning calorimetry (DSC), and the thermal stability to the LC alignment on that film was investigated by the annealing process and POM measurement. The polar anchoring energy characteristic of the brush-coated BiAlGaSnO film was examined by capacitance–voltage characteristic analysis. To examine the applicability of the brush-coated film in twisted nematic (TN) LC systems, the EO characteristics such as RT were observed.

2. Experimental

2.1 Production of the BiAlGaSnO film by the brush coating method

The BiAlGaSnO solution was produced *via* sol-gel processing; a 0.1 M solution containing bismuth(III) nitrate pentahydrate, ACS

reagent, $\geq 98.0\%$ $[\text{Bi}(\text{NO}_3)_3 \cdot 5\text{H}_2\text{O}]$, aluminum nitrate nonahydrate $[\text{Al}(\text{NO}_3)_3 \cdot 9\text{H}_2\text{O}]$, gallium(III) nitrate hydrate $[\text{Ga}(\text{NO}_3)_3 \cdot x\text{H}_2\text{O}]$, and tin(II) chloride, $\geq 99.99\%$ (trace metal basis) $[\text{SnCl}_2]$, was dissolved in 2-methoxyethanol (2ME) at the same ratio. One drop each of monoethanolamine and acetic acid was added as stabilizers. The mixed solution was stirred at 450 rpm for 2 h at 80 °C and aged for at least 1 day. Then, glass substrates were rinsed using acetone, isopropyl alcohol, and deionized water with ultrasonication for 10 min each and dried with N_2 gas. The prepared brush hairs were deeply wetted in the prepared BiAlGaSnO solution and combed over the glass substrate to form the BiAlGaSnO oriented film. Fig. 1 illustrates the brush coating process and its expected surface orientation. The coated BiAlGaSnO films were cured at 80 °C, 180 °C, and 280 °C for 1 h each.

2.2 LC alignment state and EO performance investigations of the BiAlGaSnO film

The antiparallel LC cells were formed based on the BiAlGaSnO films with gaps of 60 μm . The positive LCs (IAN-5000XX T14, $\Delta n = 0.111$, $n_e = 1.595$, $n_o = 1.484$; JNC) in the nematic phase were poured using a syringe by capillary force at room temperature (about 25 °C). The LCs have a clearing point of 81.8 °C. Then, POM (BXP 51, Olympus) measurements were conducted to confirm the LC alignment state. The pretilt angle analysis was also performed *via* the crystal rotation method (Autronic TBA 107) to demonstrate the LC alignment properties. The thermal stability test of the LC molecules on the BiAlGaSnO film was conducted by annealing from 90 to 180 °C at intervals of 30 °C with observations of the LC alignment *via* POM. To examine the anchoring energy characteristics, the LC cell with a 5 μm uniform cell gap was fabricated at room temperature, and the capacitance–voltage graph was plotted (LCR meter, Agilent 4284A). To estimate the EO characteristics, TN-LC cells were prepared on the BiAlGaSnO films with a 5 μm cell gap. The RT *versus* transmittance graphs were measured using an LCD evaluation system (LCMS-200).

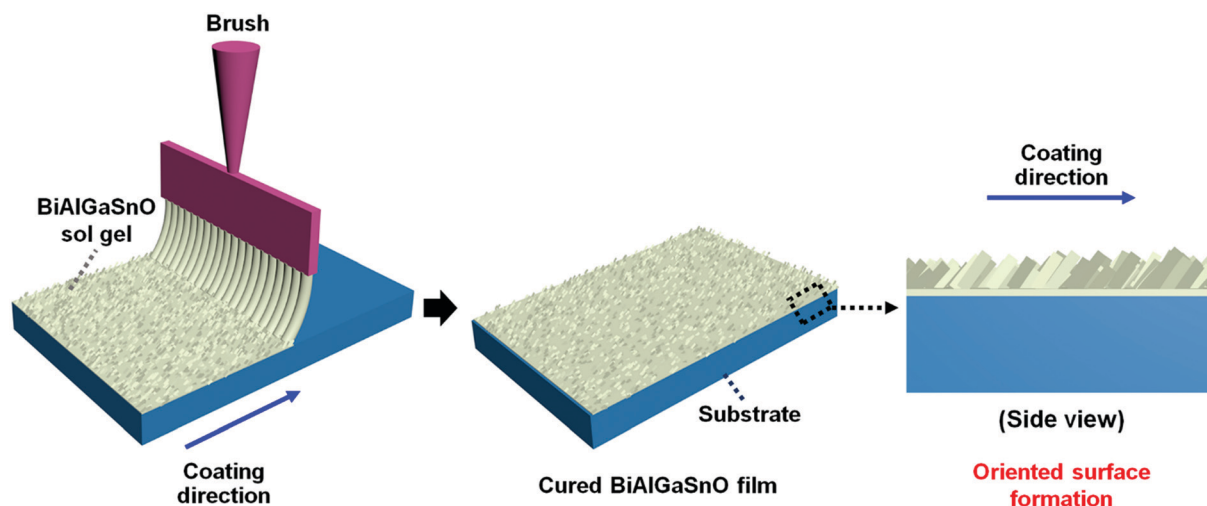


Fig. 1 Illustration of the brush coating process of the bismuth aluminum gallium tin oxide (BiAlGaSnO) thin film. A deeply wetted brush (in BiAlGaSnO solution) was used to comb the glass substrate and an oriented structure composed of BiAlGaSnO could be observed after curing.



2.3 Surface property investigation of the brush-coated BiAlGaSnO film

To investigate the stoichiometric properties of the brush-coated BiAlGaSnO film, XPS (K-alpha, Thermo Scientific) was performed using a 12 kV/3 mA power source and a monochromatic Al X-ray source (Al K α line: 1486.6 eV). To investigate the surface morphological characteristics, AFM (NX-10, Park Systems) analysis was performed. The film thickness was measured using a DektakXT stylus profiler (Bruker) with a 2 μ m radius tip and a 3 mg stylus force. The surface chemical affinity was analyzed *via* contact angle measurements of one drop each of deionized water and diiodomethane. A Phoenix 300 surface angle analyzer and IMAGE PRO 300 software were used for this purpose. The surface crystalline structure properties were observed by XRD (DMAX-IIIA, Rigaku) and TEM-SAD (200 kV accelerating voltage, JEM-F200) analyses. DSC (DSC 8000, PerkinElmer) analysis was conducted to investigate the thermal characterization of BiAlGaSnO using an aluminum pan (PerkinElmer). The starting temperature was set at 30 $^{\circ}$ C and the temperature was increased at a heating rate of 10 $^{\circ}$ C min $^{-1}$ under 20 mL min $^{-1}$ N $_2$ gas. The final temperature was set at 450 $^{\circ}$ C.

3. Results and discussion

To investigate the alignment of the LCs on the BiAlGaSnO films, AP LC cells were fabricated using BiAlGaSnO films cured at 80 $^{\circ}$ C, 180 $^{\circ}$ C, and 280 $^{\circ}$ C. The fabricated LC cells were measured using POM, and the results are presented in Fig. 2(a). When the polarizer and analyzer were vertically crossed, the 80 $^{\circ}$ C cured film represented a broadly distributed bright yellow image, which indicates the randomly distributed LC alignment state. The film cured at 180 $^{\circ}$ C also showed a yellow image but had slightly improved quality, in that it was closer to a black image. On the other hand, the film cured at 280 $^{\circ}$ C exhibited a complete and vivid dark image, indicating a uniformly aligned LC state on the film. The uniformly aligned LCs can guide the light direction uniformly when light passes through the fabricated AP LC cells. Therefore, when the polarizer and analyzer above and below the LC cell are perpendicular to each other, the POM results show a dark image (indicating no light leakage). The light path and blocking mechanism when light passes through the AP LC cell show that the LC molecules are aligned uniformly, as illustrated in Fig. 2(b). From the POM results, it is proved that the LC alignment state on the brush-coated BiAlGaSnO film could be affected by the curing temperature and that the 280 $^{\circ}$ C cured BiAlGaSnO film has uniform LC alignment.

To investigate the LC alignment state in greater detail, the pretilt angles of the LCs in the fabricated AP LC cells were measured, as shown in Fig. 3, *via* the crystal rotation method by observing the transmittance curves *versus* latitudinal rotation angles from -70° to $+70^{\circ}$.³¹ The 80 $^{\circ}$ C cured BiAlGaSnO film, which showed a nonuniform alignment state in the POM results, represents an irregular transmittance curve (red lines indicate the measured experimental data and blue lines

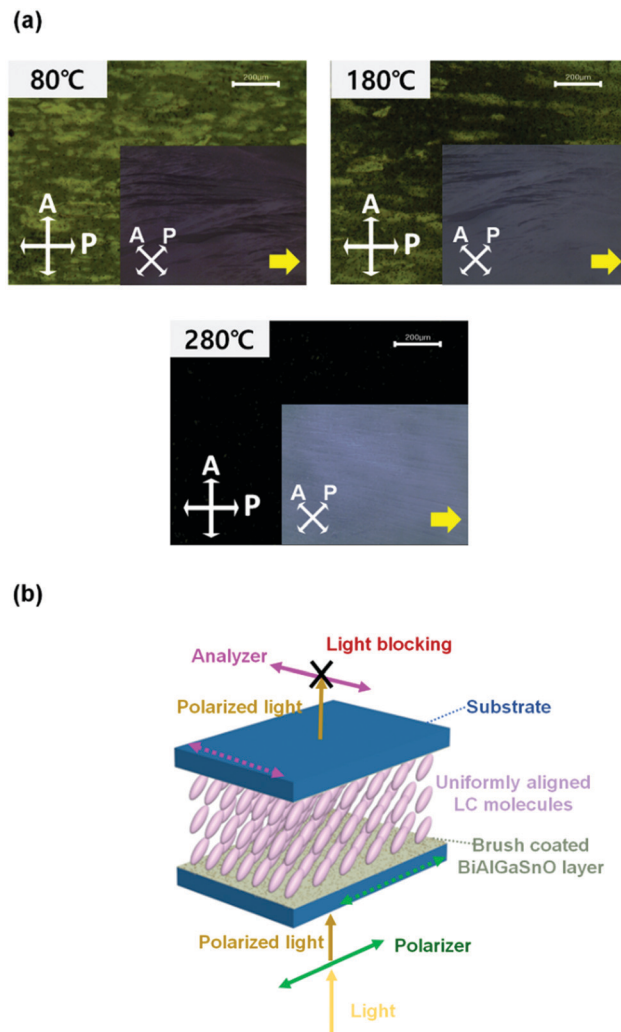


Fig. 2 (a) Liquid crystal (LC) alignment state investigation *via* polarized optical microscopy images. The antiparallel LC cells on the brush coated bismuth aluminum gallium tin oxide films (cured at 80 $^{\circ}$ C, 180 $^{\circ}$ C, and 280 $^{\circ}$ C) were observed. The analyzer (A) and polarizer (P) directions are indicated by white arrows. The brush-coating direction is represented by thick yellow arrows. (b) Illustration of the light path and blocking mechanism when passing through an antiparallel LC cell in which the LC molecules are uniformly aligned. The brush-coated bismuth aluminum gallium tin oxide film is used for the alignment layer and the analyzer and polarizer are vertically crossed.

indicate the simulation data). This film also showed an extremely low match rate with the simulation data, indicating the instability of the film. It can be assumed that this is the effect of the residual solvent based on the low curing temperature, and the calculated pretilt angles have large deviations, indicating low reliability. The 180 $^{\circ}$ C cured film shows an improved match rate with the simulation data but the transmittance curve is still irregular. This film-based LC cell showed a close to zero pretilt angle, which denotes the homogeneous alignment state of the LCs. The 280 $^{\circ}$ C cured film exhibits an extremely high match rate between the experimental and simulation data. Very small deviations are observed, indicating a stable film state. Similarly, this film shows homogeneous LC alignment. Thus, it was



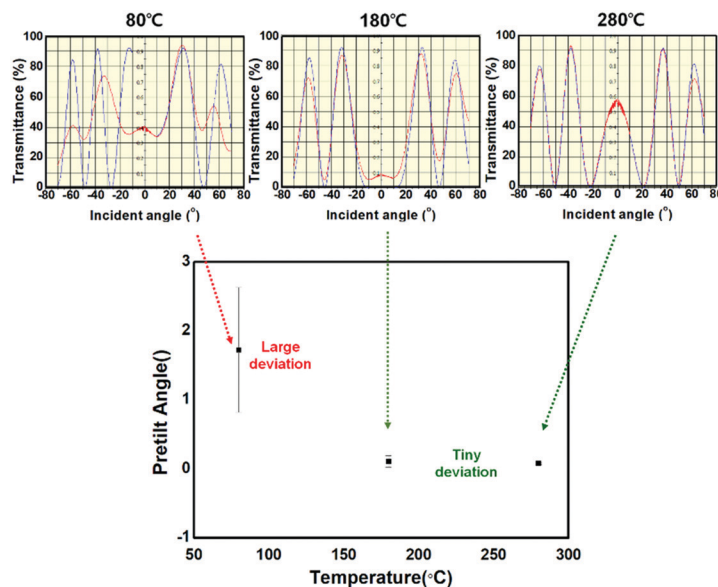


Fig. 3 Pretilt angle measurements *via* oscillated transmittance graphs obtained by the crystal rotation method. The measured sample antiparallel LC cells were prepared from the brush-coated bismuth aluminum gallium tin oxide films cured at 80 °C, 180 °C, and 280 °C.

proven that the brush-coated BiAlGaSnO film could achieve uniform and homogeneous LC alignment.

The film thickness of the brush-coated BiAlGaSnO film was obtained as 190 nm from the DektakXT analysis, and the surface morphological characteristics of the films were investigated by AFM, as shown in Fig. 4(a). The 80 °C cured film showed irregular lumps without orientation, and the lumps were induced by agglomeration of the BiAlGaSnO sol-gel with the residual solvent. This characteristic does not affect the orientation of the LCs on the film. The 180 °C cured film also shows irregular lumps, but with orientation in the same direction as the brush coating. This can somewhat affect the orientation of the LCs on the film, but the irregularity prevents achieving uniform LC alignment. With these irregular large lumps, the surface root-mean-square roughness values of the 80 °C and 180 °C cured films were obtained as 35.2 nm and 57.0 nm, respectively. On the other hand, the 280 °C cured film exhibits regular lumps with orientation in the same direction as the brush coating. During the brush coating process, since an effective contact is maintained between the brush hairs and the BiAlGaZnO solution, a constant shear stress can occur over the entire depth of the solution.³² This is attributed to the two boundaries formed between the brush hairs and the solution and between the solution and the substrate.³³ This directional structure formation through brush coating has been reported before.³⁴ When the anisotropic distribution of the BiAlGaSnO precursor occurred *via* brush coating before curing, the sol state of BiAlGaSnO was transformed into a gel state through a subsequent curing process and the BiAlGaSnO film was fabricated. During this process, the sufficient thermal energy transfer can contribute to the formation of a film structure while maintaining the anisotropy and directionality of the brush-coated BiAlGaSnO. Therefore, the orientational structure was

observed on the surface under higher curing conditions (280 °C, in this case). With this orientational structure, the surface root-mean-square roughness value of the 280 °C cured film was measured to be 4.4 nm. For specific analysis, the line profiles of the brush-coated BiAlGaSnO film surfaces were further investigated, as shown in Fig. 4(b). The film surfaces cured at 80 and 180 °C showed irregular morphologies without any distinct characteristics. However, the film cured at 280 °C showed increased heights of the surface structures, followed by a decrease, and repeated along the brush coating direction, thus supporting the directional structure noted in the morphological images. The structure had a height of 10 nm and a periodicity of 740 nm. For the uniform LC alignment, the physical anisotropic property of the alignment layer must be ensured, which can be produced by structures aligned in a single direction, such as microgrooves.^{35,36} This anisotropic surface can affect the orientations of the LCs on the film because of their collective behavior property and characteristic of minimizing elastic distortion. This surface creates geometric constraints under the boundary condition of the interface with the LCs. In Berreman's model, the LC molecules are aligned homogeneously in the surface groove when an anisotropic boundary occurs in that groove. This anisotropic boundary effect of the groove to LCs has been previously reported.^{37–39} These AFM results correspond with the results of the POM and pretilt angle analyses.

To investigate the chemical composition and ensure the formation of the BiAlGaSnO film on the substrate, the Al 2p, Bi 4f, Ga 2p, Sn 3d, and O 1s core-level XPS measurements were performed on the brush-coated BiAlGaSnO films cured at 80 and 280 °C, as shown in Fig. 5. The Al 2p spectra showed single peaks centered at 74.0 and 74.66 eV binding energies for the films cured at 80 and 280 °C, respectively. The peaks indicate



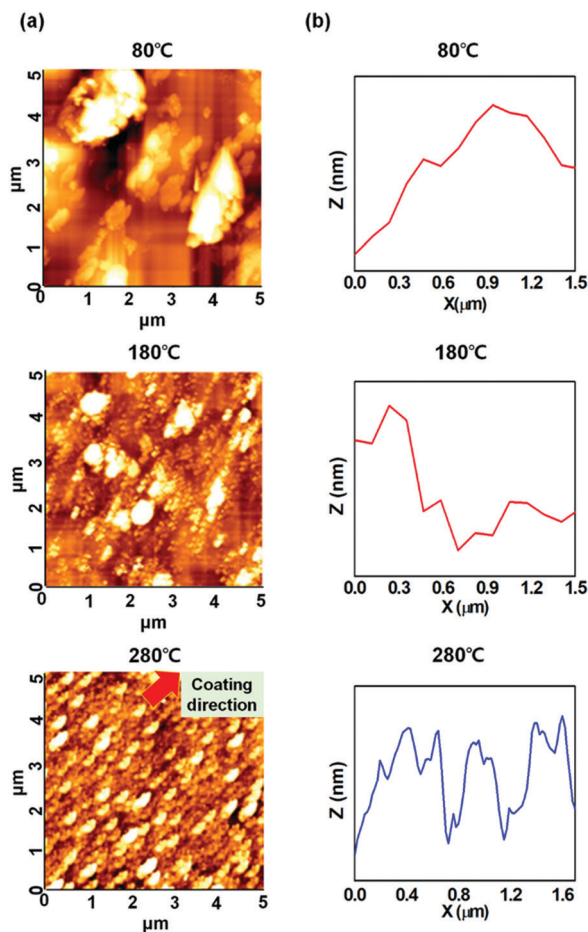


Fig. 4 (a) Morphological images of brush-coated bismuth aluminum gallium tin oxide (BiAlGaSnO) films cured at 80 °C, 180 °C, and 280 °C obtained by atomic force microscopy. The brush coating direction is denoted by the red arrow. (b) Line profiles of brush-coated BiAlGaSnO films cured at 80, 180, and 280 °C.

the oxidized states of aluminum, and the increased peak at 280 °C implies active thermal oxidation on the film. The Bi 4f spectrum showed four peaks centered at 158.06, 159.32, 163.45, and 164.62 eV binding energies for the film cured at 80 °C, indicating the Bi 4f_{7/2} metal, Bi 4f_{7/2} oxide, Bi 4f_{5/2} metal, and Bi 4f_{5/2} oxide, respectively. On the other hand, for the film cured at 280 °C, two peaks centered at 159.66 and 164.94 eV binding energies were observed, indicating Bi 4f_{7/2} and Bi 4f_{5/2} oxides, respectively. This indicates the incomplete oxidation state of the film cured at 80 °C and the fully oxidized state of Bi on the film cured at 280 °C. The Ga 2p spectra exhibited two peaks in films cured at both temperatures, which were centered at 1117.66 and 1144.41 eV for the film cured at 80 °C and at 1117.99 and 1144.76 eV for the film cured at 280 °C, indicating Ga 2p_{3/2} and Ga 2p_{1/2}, respectively. Similarly, in the Al 2p spectrum, the increased intensity of the film cured at 280 °C indicates the active thermally oxidized Ga state. The Sn 3d spectrum displayed three peaks centered at 486.38, 494.84, and 496.94 eV binding energies for the film cured at 80 °C, which indicate Sn 3d_{5/2}, Sn 3d_{3/2}, and Sn–Cl bonding (induced by the

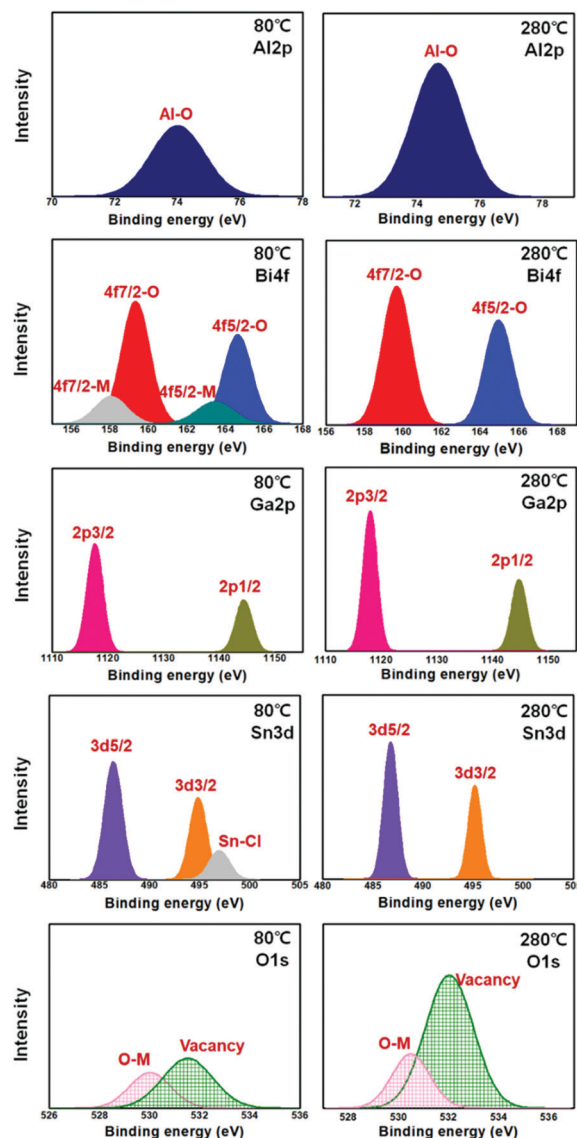


Fig. 5 Al 2p, Bi 4f, Ga 2p, Sn 3d, and O 1s core-level X-ray photoelectron spectroscopy graphs of the brush-coated bismuth aluminum gallium tin oxide films cured at 80 and 280 °C.

tin chloride material used in this study), respectively. However, the spectrum for the film cured at 280 °C only exhibited two peaks centered at 486.77 and 495.17 eV binding energies, indicating Sn 3d_{5/2} and Sn 3d_{3/2}, respectively; this indicates the fully oxidized state of Sn on these films. The O 1s spectrum showed two peaks in the films cured at both temperatures, which were centered at 530.02 and 531.52 eV binding energies for 80 °C and at 530.49 and 532.03 eV for 280 °C, indicating O–M ('M' means the metal) and oxygen vacancies, respectively. These graphs also indicate the active metal-oxidized state on the film cured at 280 °C compared to that at 80 °C. From the results, it is observed that a suitably oxidized metal state with sufficient heat is required for the directional structure that maintains the orientation of the sol state originating from the brush coating process.

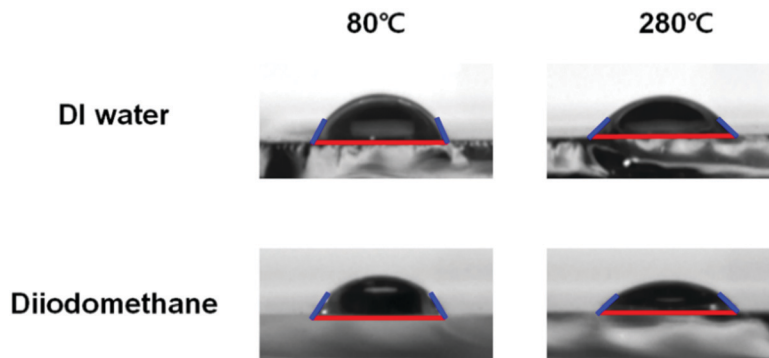


Fig. 6 Contact angle measurement images of the brush-coated bismuth aluminum gallium tin oxide films cured at 80 and 280 °C for deionized water and diiodomethane.

To investigate the chemical affinities of the brush-coated BiAlGaSnO films cured at 80 and 280 °C, the contact angles of deionized water and diiodomethane were measured, as shown in Fig. 6. Because of the some anisotropic nano-topography of the brush-coated BiAlGaSnO film as confirmed by the AFM analysis, some anisotropic drop shapes were observed. However, as shown in the figure, there was a tiny difference that was difficult to distinguish with the naked eye, and the average contact angle value was obtained. At a curing temperature of 80 °C, the contact angles of deionized water and diiodomethane were measured as 67.61° and 60.96°, respectively. On the other hand, these contact angles were measured as 48.07° and 50.89° for the film cured at 280 °C. The surface energies of the films were calculated based on the contact angles using the Owen-Wendt method,⁴⁰ and the results are presented in Table 1. As the curing temperature increased to 280 °C from 80 °C, the surface energy of the brush-coated BiAlGaSnO film increased to 55.9 from 40.82 mJ m⁻². This result indicates that, as the curing temperature increases, the brush-coated BiAlGaSnO film exhibits hydrophilic characteristics, which contributes to the homogeneous alignment of the LC molecules on the surface.

The crystalline characteristics of the brush-coated BiAlGaSnO films cured at 80, 180, and 280 °C were investigated by XRD analysis, as shown in Fig. 7(a). No specific main peaks were observed in all the XRD results of the brush-coated BiAlGaSnO films. However, some small peaks were observed at 2 theta close 42 degrees, which indicate that the solution-processed BiAlGaSn film has limited crystallinity (*i.e.*, it is not amorphous). For the specific analysis, the TEM-SAD

measurement was conducted and the results are shown in Fig. 7(b), which indicated that the solution-processed BiAlGaSnO film has a nanocrystalline structure.⁴¹ The nanocrystalline structure represents characteristics intermediate between those of amorphous and polycrystalline phases, which correspond to TEM-SAD results. The thermal analysis of BiAlGaSnO was conducted by DSC as shown in Fig. 7(c). In the DSC graph, there were some endothermic and exothermic peaks.

In particular, the endothermic peak observed at around 170 °C corresponds to the evaporation of the solvent. In the 170–182 °C range, dehydration and decomposition took place, which correspond to the elimination of the residual alcohol. The sample state continuously changed from oxidation to alloying and curing in the range of 182–320 °C, and the large exothermic peak at 190 °C is attributed to the oxidation of the material. This result corresponds to the previous analysis of that film. When the curing temperature was below 180 °C, the BiAlGaSnO film did not form properly (not oxidized fully), so the oriented structure was not constructed as intended. However, when the curing temperature was 280 °C, the BiAlGaSnO film was well formed while maintaining the directionality of the precursor with sufficient heat transfer, in which the directionality originated from the brush coating. Therefore, this BiAlGaSnO film could be applied to the LC alignment layer.

To investigate the thermal stability to the LC alignment on the brush-coated BiAlGaSnO film, the LC cells fabricated with the film cured at 280 °C were observed using POM at various annealing temperatures, as shown in Fig. 8. The annealing temperature was increased from 90 °C to 180 °C at 30 °C intervals for 10 min at each value. Below 180 °C, the POM analysis showed vivid dark images, which means a uniform LC alignment state in the LC cells. On the other hand, for the 180 °C condition, the POM image displayed defects, indicating nonuniform LC alignment. From the results, it was observed that the brush-coated BiAlGaSnO film cured at 280 °C exhibits suitable thermal stability for LC alignment, which is an important factor for advanced LC device applications that accompany numerous switching operations.

To examine the applicability of the brush-coated BiAlGaSnO films cured at 280 °C in TN LCDs, the EO characteristics of the

Table 1 Contact angle measurement results and the obtained surface energies of the brush-coated bismuth aluminum gallium tin oxide films cured at 80 and 280 °C

| Curing temperature (°C) | Contact angle (°) | | Dispersive energy (mJ m ⁻²) | Polar energy (mJ m ⁻²) | Surface energy (mJ m ⁻²) |
|-------------------------|-------------------|---------------|---|------------------------------------|--------------------------------------|
| | DI* water | Diiodomethane | | | |
| 80 | 67.61 | 60.96 | 28.02 | 12.8 | 40.82 |
| 280 | 48.07 | 50.89 | 33.78 | 22.12 | 55.9 |

*Deionized.



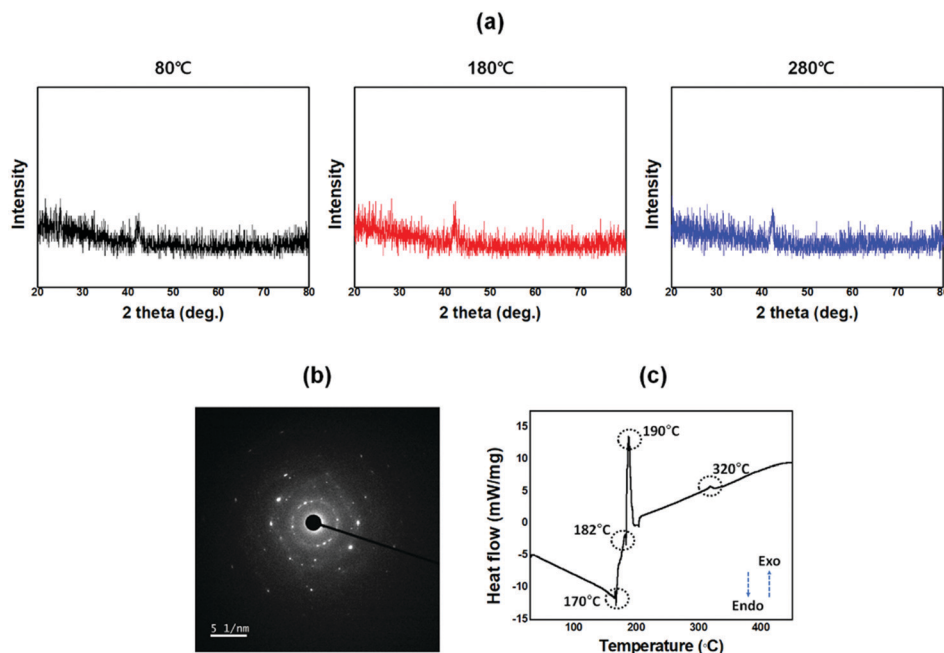


Fig. 7 (a) X-ray diffraction results of the brush-coated bismuth aluminum gallium tin oxide (BiAlGaSnO) films cured at 80, 180, and 280 °C. (b) Transmission electron microscopy selected area diffraction image for the BiAlGaSnO film on a Cu–C grid. (c) Differential scanning calorimetry graph of the BiAlGaSnO film in the temperature range of 30 °C to 450 °C.

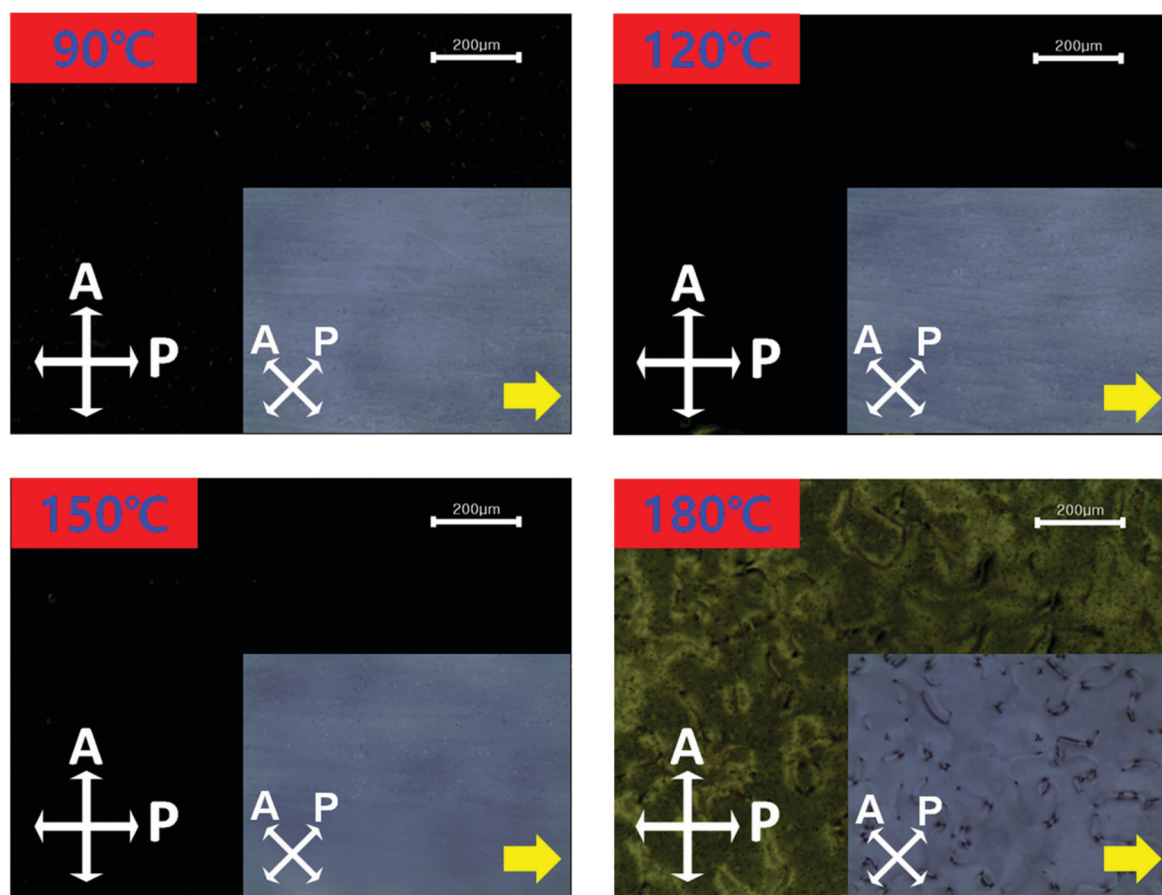


Fig. 8 Thermal stability investigation using polarized optical microscopy. The antiparallel cells were assembled on the brush coated bismuth aluminum gallium tin oxide films cured at 280 °C. The annealing temperature was increased from 90 °C to 180 °C at 30 °C intervals for 10 min at each value.



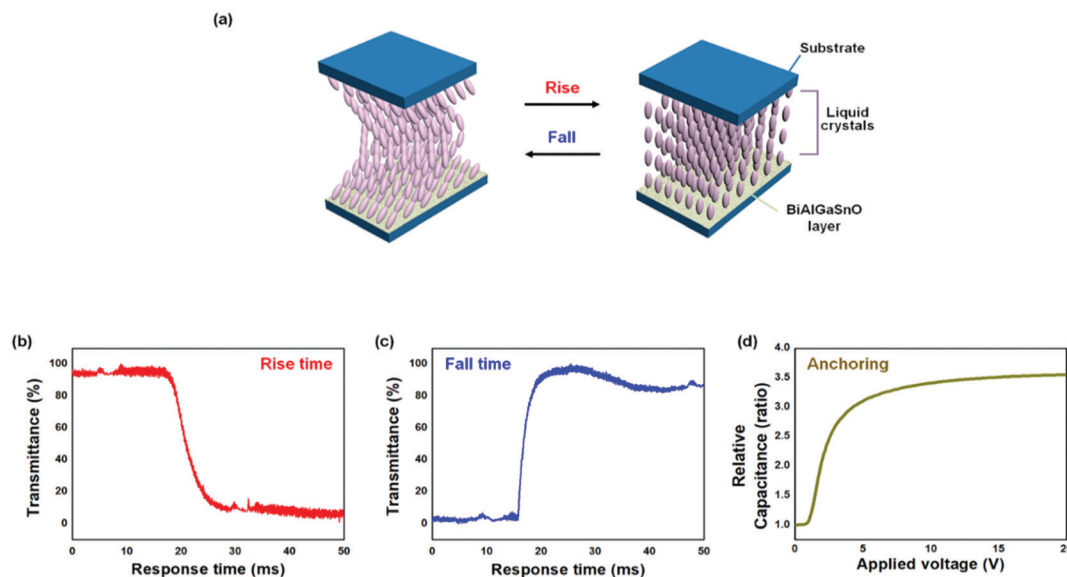


Fig. 9 (a) Illustration of liquid crystal (LC) alignment state transitions in the twisted-nematic LC system. (b) Rise and (c) fall times of the twisted-nematic LC cells fabricated from the brush-coated bismuth aluminum gallium tin oxide (BiAlGaSnO) film cured at 280 °C. (d) Anchoring energy characteristic of the LC cell assembled by brush-coated BiAlGaSnO films cured at 280 °C.

fabricated TN LC cells were estimated. In the TN LC system, the rise time indicates the LC transition time from the lying down to the standing state, and the fall time denotes the transition time for the opposite condition, as illustrated in Fig. 9(a). The twisted LCs in the lying down state transmit the light passing through the cell by rotating the light direction by 90°; in the standing LC state, the light passing through the cells is blocked by the polarizers located above and below the LC cell and rotated 90° from each other. The rise time of the TN cells based on the brush-coated BiAlGaSnO film was measured as 8.6 ms from Fig. 9(b), and the fall time was measured as 3.3 ms from Fig. 9(c). The total response time was calculated as 11.9 ms, which indicates the fast switching performance of the brush-coated BiAlGaSnO alignment layer compared to the conventionally used polyimide layer.⁴² The anchoring energy characteristic was examined as shown in Fig. 9(d). From the voltage-capacitance graph, the anchoring energy of the brush-coated BiAlGaSnO film cured at 280 °C was measured to be $2.45 \times 10^{-4} \text{ J m}^{-2}$. It shows the competitiveness of the film because the corresponding value of the conventionally used PI layer is in the range of 10^{-4} – 10^{-5} J m^{-2} .⁴³ From the above results, it is demonstrated that the brush-coated BiAlGaSnO film can be applied to TN-LCDs with competitive switching properties.

4. Conclusions

Herein, we demonstrate a very simple coating process using brush hairs that simultaneously achieves alignment treatment for LCs. This simplification of operations makes it possible to expect a high throughput. The brush-coated BiAlGaSnO film was used in the alignment layer, and a uniform and homogeneous alignment state was confirmed by POM and pretilt

angle analyses. The physicochemical characteristics of the BiAlGaSnO film were investigated by AFM and XPS analyses. The XPS results showed a well-formed BiAlGaSnO layer, and the AFM results showed an oriented structure for the brush-coated BiAlGaSnO surface cured at 280 °C. This oriented structure provides geometric constraints to the LCs on the surface, such as microgrooves, and results in a uniform LC alignment state. The BiAlGaSnO surface shows hydrophilic characteristics in the contact angle analysis and a nanocrystalline structure in the TEM-SAD analysis. The thermal endurance to the LC alignment of the BiAlGaSnO film was verified by the annealing process and showed a superior thermal budget for up to 150 °C. The EO characteristics of the brush-coated BiAlGaSnO film cured at 280 °C were proved for the fabricated TN LC cells, which showed fast switching. From the above results, we expect that the brush coating method could be adopted for next-generation LC devices.

Conflicts of interest

There are no conflicts to declare.

Acknowledgements

The authors acknowledge the financial support from Shanghai Sailing Program (Grant No. 18YF1400900) and the Natural Science Foundation of Shanghai (Grant No. 22ZR1401400).

Notes and references

- 1 X. Yan, F. W. Mont, D. J. Poxson, M. F. Schubert, J. K. Kim, J. Cho and E. F. Schubert, *Jpn. J. Appl. Phys.*, 2009, **48**, 120203.



- 2 S. Bulja, D. Mirshekar-Syahkal, R. James, S. E. Day and F. A. Fernández, *IEEE Trans. Microwave Theory Tech.*, 2010, **58**, 3493.
- 3 M. S. Zakerhamidi, M. H. M. Ara and A. Maleki, *J. Mol. Liq.*, 2013, **181**, 77.
- 4 Y. Chen, D. Xu, S.-T. Wu, S. Yamamoto and Y. Haseba, *Appl. Phys. Lett.*, 2013, **102**, 141116.
- 5 Y. Garbovskiy, *Appl. Phys. Lett.*, 2016, **108**, 121104.
- 6 J.-J. Lee, H.-G. Park, J.-J. Han, D.-H. Kim and D.-S. Seo, *J. Mater. Chem. C*, 2013, **1**, 6824.
- 7 W.-K. Lee, Y.-S. Choi, Y.-G. Kang, J. Sung, D.-S. Seo and C. Park, *Adv. Funct. Mater.*, 2011, **21**, 3843.
- 8 Y. Ji, F. Fan, Z. Zhang, J. Cheng and S. Chang, *Carbon*, 2022, **190**, 376.
- 9 S.-W. Oh and T.-H. Yoon, *Opt. Express*, 2014, **22**, 5808.
- 10 Y. C. Su, C. C. Chiou, V. Marinova, S. H. Lin, N. Bozhinov, B. Blagoev, T. Babeva, K. Y. Hsu and D. Z. Dimitrov, *Opt. Quantum Electron.*, 2018, **50**, 205.
- 11 R. Hong, J. Shao, H. He and Z. Fan, *Appl. Surf. Sci.*, 2006, **252**, 2888.
- 12 F. Chen, Y. Xia, Q. Lv, S. Mao and Y. Li, *J. Phys. Chem. C*, 2022, **126**, 1099.
- 13 Z. J. Ren, X. Zhang, H. H. Li, X. L. Sun and S. K. Yan, *Chem. Commun.*, 2016, **52**, 10972.
- 14 T. Zhu, K. Shanmugasundaram, S. C. Price, J. Ruzyllo, F. Zhang, J. Xu, S. E. Mohny, Q. Zhang and A. Y. Wang, *Appl. Phys. Lett.*, 2008, **92**, 023111.
- 15 C. Jiang, Z. Zhong, B. Liu, Z. He, J. Zou, L. Wang, J. Wang, J. Peng and Y. Cao, *ACS Appl. Mater. Interfaces*, 2016, **8**, 26162.
- 16 M. M. Ovhall, N. Kumar, S. Lim and J.-W. Kang, *Appl. Surf. Sci.*, 2020, **529**, 147072.
- 17 A. Vital, M. Vayer, T. Tillocher, R. Dussart, M. Boufnichel and C. Sinture, *Appl. Surf. Sci.*, 2017, **393**, 127.
- 18 X. Wu, S. Lan, G. Zhang, Q. Chen, H. Chen and T. Guo, *Adv. Funct. Mater.*, 2017, **27**, 1703268.
- 19 M. Zhang, B. Hu, L. Meng, R. Bian, S. Wang, Y. Wang, H. Liu and L. Jiang, *J. Am. Chem. Soc.*, 2018, **140**, 8690.
- 20 L. Li, T. Yang, K. Wang, H. Fan, C. Hou, Q. Zhang, Y. Li, H. Yu and H. Wang, *J. Colloid Interface Sci.*, 2021, **583**, 188.
- 21 C. Guo, X. Gao, F.-J. Lin, Q. Wang, L. Meng, R. Bian, Y. Sun, L. Jiang and H. Liu, *ACS Appl. Mater. Interfaces*, 2018, **10**, 39448.
- 22 M. Ito, K. Kajiwarra and K. Takatoh, *Jpn. J. Appl. Phys.*, 2022, **61**, 012004.
- 23 O. Yaroshchuk, R. Kravchuk, A. Dobrovolsky, L. Qiu and O. D. Lavrentovich, *Liq. Cryst.*, 2004, **31**, 859.
- 24 P. Wen, R. He, X.-D. Li and M.-H. Lee, *J. Mater. Sci.*, 2022, **57**, 755.
- 25 E. A. P. van Heijst, S. E. T. ter Huurne, J. A. H. P. Sol, G. W. Castellanos, M. Ramezani, S. Murai, M. G. Debije and J. G. Rivas, *J. Appl. Phys.*, 2022, **131**, 083101.
- 26 J. V. Haaren, *Nature*, 2001, **411**, 29.
- 27 S. B. Jang, G.-S. Heo, E.-M. Kim, H.-G. Park, J. H. Lee, Y. H. Jung, H.-C. Jeong, J.-M. Han and D.-S. Seo, *Liq. Cryst.*, 2016, **43**, 285.
- 28 H.-C. Jeong, J. H. Lee, D. H. Kim, D. W. Lee, J. M. Han, B.-Y. Oh, T. W. Kim and D.-S. Seo, *Liq. Cryst.*, 2019, **46**, 86.
- 29 I. H. Song, H.-C. Jeong, J. H. Lee, J. Won, D. H. Kim, D. W. Lee, J. Y. Oh, J. I. Jang, Y. Liu and D.-S. Seo, *Adv. Opt. Mater.*, 2021, **9**, 2001639.
- 30 M. Ceh, H.-C. Chen, M.-J. Chen, J.-R. Yang and M. Shiojiri, *Mater. Trans.*, 2010, **51**, 219.
- 31 K. Y. Han, T. Miyashita and T. Uchida, *Mol. Cryst. Liq. Cryst. Sci. Technol., Sect. A*, 1994, **241**, 147.
- 32 C. C. Mell and S. R. Finn, *Rheol. Acta*, 1965, **4**, 260.
- 33 S.-S. Kim, S.-I. Na, J. Jo, G. Tae and D.-Y. Kim, *Adv. Mater.*, 2007, **19**, 4410.
- 34 F.-J. Lin, C. Guo, W.-T. Chuang, C.-L. Wang, Q. Wang, H. Liu, C.-S. Hsu and L. Jiang, *Adv. Mater.*, 2017, **29**, 1606987.
- 35 H. Kikuchi, J. A. Logan and D. Y. Yoon, *J. Appl. Phys.*, 1996, **79**, 6811.
- 36 B. Chae, S. B. Kim, S. W. Lee, S. I. Kim, W. Choi, B. Lee, M. Ree, K. H. Lee and J. C. Jung, *Macromolecules*, 2002, **35**, 10119.
- 37 D. W. Berreman, *Phys. Rev. Lett.*, 1972, **28**, 1683.
- 38 J.-I. Fukuda, M. Yoneya and H. Yokoyama, *Phys. Rev. Lett.*, 2007, **98**, 187803.
- 39 Y. Choi, H. Yokoyama and J. S. Gwag, *Opt. Express*, 2013, **21**, 12135.
- 40 A. W. Adamson, *Physical Chemistry of Surfaces*, Wiley-Interscience, New York, 1990.
- 41 S. Y. Kim, H.-G. Park, M.-J. Cho, H.-C. Jeong and D.-S. Seo, *Liq. Cryst.*, 2014, **41**, 940.
- 42 Y. Liu, J. H. Lee and D.-S. Seo, *Opt. Express*, 2016, **24**, 17424.
- 43 J. H. Lee, H.-C. Jeong, J. Won, B.-Y. Oh, D. H. Kim, D. W. Lee, Y. Liu and D.-S. Seo, *Polymer*, 2019, **161**, 1.

